University of Nevada, Reno

Development of a Model System for Culturing Neonatal Rat Ventricular Myocytes *in vitro* to Monitor Integrin Activation in Response to Altered Contractile Force

A thesis submitted in partial fulfillment of the

requirements for the degree of Master of Science in

Biochemistry

By

Amanda M.Cline

Dr. Maria Valencik/ Thesis Advisor

August 2011

University of Nevada, Reno
Statewide • Worldwide

THE GRADUATE SCHOOL

We recommend that the thesis
prepared under our supervision by

AMANDA M. CLINE

entitled

Development Of A Model System For Culturing Neonatal Rat Ventricular Myocytes In Vitro To Monitor Integrin Activation In Response To Altered Contractile Force

be accepted in partial fulfillment of the
requirements for the degree of

MASTER OF SCIENCE

Maria Valencik, Advisor

Robert Harvey, Committee Member

Josh Baker, Committee Member

Normand Leblanc, Graduate School Representative

Marsha H. Read, Ph. D., Dean, Graduate School

August, 2011

Abstract:

Hypertrophic cardiomyopathy (HCM) affects 1 in 500 individuals and remains the leading cause of sudden cardiac death (SCD) in young adults. Recent evidence links mutations within sarcomeric proteins to the HCM disease state. The interplay between the forces generated by the contractile apparatus and sensed by integrins is central to understanding the pathogenesis of HCM. Integrins are likely the mechanotransducers in cardiomyocytes, converting mechanical stress into chemical signals that stimulate cardiac hypertrophy. Outside-in integrin signaling has been extensively studied, while inside-out signaling in response to changes in contractile force remains undefined. An in vitro culture of cardiomyocytes exhibits disorganization of myofibril structure and intercalated disc formation, making it difficult to determine the physiological relevance. Therefore, we have developed an in vitro tissue model to mimic in vivo physiology. Specifically, we have developed a flexible micropatterned scaffold to better mirror native ECM and allow more meaningful correlation of findings to living systems. The micropatterned laminin matrix allows organized growth and differentiation of neonatal rat ventricular myocytes (NRVMs) into adult phenotype. We have constructed an adenovirus expressing a talin-GFP fusion protein to monitor integrin activation in response to changes in contractile force. We have confirmed talin-GFP colocalization with integrins at cell-ECM contacts using confocal microscopy. Utilizing total internal fluorescence (TIRF) microscopy we have completed preliminary measurements of intensity changes overtime at focal adhesions. Utilizing ImageJ technology, we aim to determine how changes in acto-myosin force affect integrin activation by measuring the changes in focal adhesion intensity, as observed through GFP localization.

We hypothesize that mutations and inhibition of sarcomere contractile elements will cause perturbations in traction forces and alter inside-out integrin signaling, initiating a pathological hypertrophic phenotype.

Acknowledgements:

Thanks to Dr. Maria Valencik, Mariam Ba, and Iva Neaveux for help with cardiomyocyte protocols and various other aspects of the project. Thank you to the Baker lab for their contributions to this project. Thank s to our undergraduate team that worked tirelessly on many aspects of this project; Amrita Kaur, Michael Fears, and Jeffrey Surina.

Table of Contents

List of Figures

Introduction:

Cardiac Hypertrophy:

Heart failure is one of the leading causes of mortality in the western world and includes a wide variety of cardiac pathologies. Hypertrophic cardiomyopathy is the leading cause of sudden cardiac death in children and young adults, often seen in the sudden death of young athletes (Agrawal, et al. 2009). Hypertrophy is initially seen to be beneficial to the heart as it compensates for the increased stress placed upon the organ; cardiac myocytes undergo an increase in cell size to maintain standard cardiac output. But, sustained hypertrophy causes the heart to become decompensated and leads to overt heart failure (Ruwhof and van der Laarse 2000, Clerk, et al. 2007). During sustained hypertrophy we see a switch from cardiac α-actin to skeletal α-actin and from the α-form of myosin heavy chain to the β-MHC form in rodents (Schwartz, et al. 1986).

Pathological hypertrophy causes increased heart size that is originally compensatory, but can lead to declined left ventricular function and represents an independent risk factor for heart failure. Physiological hypertrophy is seen in healthy individuals following pregnancy or exercise and is not associated with cardiac damage (Barry, Davidson and Townsend 2008). Cardiac myocytes in the adult heart do not divide (Nadal-Ginard, et al. 2003), leaving the heart vulnerable to pathophysiological stresses such as hypoxia and/or apoptosis. Surviving cardiomyocytes are forced to accommodate an increase in workload and undergo hypertrophic growth to maintain cardiac function. (Dorn, Robbins and Sugden 2003). Heart failure caused by hypertrophic growth remains a poorly understood mechanism where the heart can no

longer compensate for the sustained pressure overload (Johnston, et al. 2009). Cell death can be a mechanism for the development of heart failure and increased levels of cells death has been noted in heart failure patients (Wenker, et al. 2003, Narula, et al. 1996, Johnston, et al. 2009).

Integrins:

Integrins are heterodimeric transmembrane receptors composed of α and β subunits (Arnaout, Goodman and Xiong 2007, Hynes 1987). Presently, 22 heterodimers have been identified composed of 16α and 8β chains. Integrins have the ability to function bidirectionally. The cytoplasmic tails allow integrins to bind to a range of cytoskeletal molecules; for example the binding of talin to integrin tails produces a change in integrin affinity for ligands (Calderwood, et al. 1999, Bouaouina, Lad and Calderwood 2008). Integrins are essential for the interaction between the extracellular matrix and cardiac myocytes and fibroblasts. They are vital in modulating processes such as cell survival, cell migration, remodeling the cytoskeleton, and the formation of focal adhesions. The activation of integrins is important in many biological processes including embryonic development (Hughes and Pfaff 1998), hemostasis (Bennett and Vilaire 1979), and angiogenesis (Byzova, et al. 2000). They also transmit signals through organizing the cytoskeleton which leads to stabilization of cell adhesions and regulating the shape, morphology, and motility of the cell (Ruwhof and van der Laarse 2000, Ingber 1991). The affinity and avidity of the integrin ectodomain are controlled by the cytoskeleton, which allows integrin to modulate the extracellular matrix. When integrin

binds to the extracellular matrix, the cytoskeleton may change shape or composition in response.

Integrins are unique in their ability to sense changes in physiological and pathophysiological signals in the heart, known as mechanotransduction (Inger 1998, Simpson 1999, Chen 2008). Bidirectional signaling in integrins is composed of both inside-out and outside-in signaling. During outside-in signaling, ligands bind the extracellular head of integrins causing a cascade of intracellular signaling events leading to changes in cell morphology, migration, proliferation, differentiation, survival, and gene expression. The ability of integrins to bind to ligands is directly regulated by cellular signaling mechanisms known as activation or inside out signal transduction (Carman and Springer 2003, Shimaoka, Takagi, and Springer 2002, Liddington and Ginsberg 2002). Inside-out signaling is characterized by binding of integrin to an intracellular ligand and clustering of multiple integrins within the cell membrane occurs. Integrin clustering in cardiomyocytes is associated with chemical and mechanical signaling.

Talin:

Talin consists of an N-terminal ~50kDa globular head domain and a ~220kDa C-terminal rod domain. The head domain contains an approximate 200 residue region that is similar to the ERM domain (ezrin, radixin,and moesin) family of proteins (Rees, et al. 1990). The head domain binds to the cytoplasmic tails of integrins, while the rod domain binds to the actin cytoskeleton, thus linking the integrin to the cytoskeleton (Mangeat, Roy and Martin 1999). The rod domain also contains an integrin-binding site, vinculin

binding site, and an actin binding site. The second integrin binding site (IBS2) found in the rod domain couples integrins to the actin cytoskeleton (Moes, et al. 2007, Mangeat, Roy and Martin 1999, Hemmings, et al. 1996, Muguruma, et al. 1995)

Talin activation itself is a process that is not well understood; in some cells integrin outside-in signaling leads to the association of the large isoform of type 1 phophatidylinositol phosphate kinase and together, with talin, translocates to the plasma membrane (Moes, et al. 2007). Activation of talin is thought to relieve the autoinhibitory head-tail association seen in talin, which exposes the integrin binding site in the talin head (IBS1). Active talin, which then forms the anti-parallel homodimer, binds to and activates integrins (Moes, et al. 2007). IBS2 is the site required to link integrins to the cytoskeleton and may only interact with high affinity ligand-bound integrins (Moes, et al. 2007, Tanentzapf and Brown 2006).

Talin and Integrin:

The binding of the talin head domain to integrin β-tails is specific in that it is disrupted by single point mutations that disrupt integrin localization to talin-rich focal adhesions (Calderwood, et al. 1999). The talin head domain (THD) can bind to several integrin β tails and can mediate the linkage of integrins to the actin cytoskeleton and therefore, modulate integrin function. Both the talin head and rod domain are able to bind to the muscle-specific integrin β1D cytoplasmic tail. The binding of both the THD and the talin rod to integrins are likely to be independent interactions. .

Talin is concentrated at focal adhesions, the fact that talin can bind to integrin β cytoplasmic tails via its head domain, suggests that this interaction is involved in the

linkage of the cytoskeleton to integrins. THD is able to both bind and activate β3 integrin tails (Calderwood, et al. 1999). THD binding to the β3 integrin cytoplasmic tail is required for β3 activation, while the head is unable to activate β1 integrin tails. The F3 domain of the talin head is sufficient to bind to both the β1 and β3 tails, but is not sufficient to activate β1 tails. The F3 domain of talin binds to both the β1A and β3 tails via a conserved mechanism with a comparable affinity and it is unlikely that there is an alternate binding mechanism to explain the inability of over expressed talin fragments to activate β1 integrins (Bouaouina, Lad and Calderwood 2008). The full talin head, but not F2F3 or F3 subdomains alone, was able to activate β1 integrins. The inability of talin fragments to activate integrins is not dependent on α5 integrin cytoplasmic tail, but on the β1 tail. F2F3 was able to activate β3 integrin tails but not β1. The F1F2F3 subdomains alone (86-405) were unable to activate β1 integrins, nor was the F0 subdmain (1-86) able to do so either, indicating that these regions cooperate with one another to activate β1 integrins. On the other hand β3 integrins are activated by the expression of F2F3 or F3 alone (Calderwood, et al. 1999, Bouaouina, Lad and Calderwood 2008, Tanentzapf and Brown 2006). The F3 domain is able to activate β3 tails, but is unable to mediate the linkage of the cytoskeleton at focal complexes.

Integrins and Cardiac Hypertrophy:

Integrins are candidates as mechanotransducers in cardiomyocytes and are thought to be the link between mechanical stress and cardiac hypertrophy. Integrins are able to transduce forces created by acto-myosin contraction or changes in extracellular matrix rigidity across the plasma membrane. Integrins mediate the hypertrophic response

to external stimuli, known as passive stretch, while little is known about how changes in actin-myosin mechanics affect integrin activation and cardiac hypertrophy.

How Does a Cell Respond to Mechanical Stress?

Integrins are thought to be the mechanoreceptors that receive mechanical stress and converts it into intracellular biochemical signals. Stretching the ventricular wall as a consequence of increased aortic pressure is the mechanical parameter most closely related to an increase in protein synthesis (Kira, et al. 1984) Integrins are present in the sarcolemma and intercalated discs and are important for hypertrophic signaling. Integrin activation leads to the clustering of integrins on the cell surface and recruitment of signaling molecules onto the actin cytoskeleton to form focal adhesions, which allow for downstream signaling. Integrins are the link between the extracellular matrix and the intracellular cytoskeleton and are able to transduce both mechanical and biochemical signals across the cell.

Mechanical Stress and Cardiac Hypertrophy:

Mechanical stress is a major cause of cardiac hypertrophy. Passive stretch of cardiac myocytes activates a phosphorylation cascade of many protein kinases (I. Komuro 2000). Stretching cultured cardiomyocytes stimulated protein synthesis and induced altered gene expression, without the involvement of neural or humoral factors (Sadoshima, et al. 1992, Komuro, Kaida and Shibazaki 1990, Kira, et al. 1994, I. Komuro 2000, Mann, Kent and Cooper 1989, Vandenburg, et al. 1995). When cardiomyocytes are placed under mechanical stress the cells release growth promoting factors including angiotensin II, endothelin-1, and transforming growth factor-β (Ruwhof and van der

Laarse 2000). This stress is likely coupled to intracellular signals that are responsible for the hypertrophic response seen in these cells.

Mechanical stress-induced increases in sarcomere length changed the spatial arrangement of the desmin-laminin filament network that links Z-discs to the chromatin, which may initiate gene transcription (Bloom, Lockard and Bloom 1996)

Extracellular Matrix (ECM) and Force Generation:

Increasing force, exerted at the adhesion site by actomyosin contractility, likely exposes more talin vinculin binding sites, leading to more vinculin recruitment and thus increased actin binding (Arnaout, Goodman and Xiong 2007).Cardiomyocytes transmit actomyosin contractions through their attachments to the matrix. The elasticity of the ECM is vital to many cells and influences cell shape, protein expression and organization, and differentiation (Pelham and Wang 1997, Discher, Janmey and Wang 2005, Peyton and Putnam 2005). Cardiomyocytes isolated from neonatal rats must first attach to the substrate and then pre-myofibrils are replaced by the muscle isoforms that develop A-bands and I-Z-I bands of mature myofibrils (Engler, Carag-Krieger, et al. 2008, Ruwhof and van der Laarse 2000).

Mechanical compliance of the matrix is becoming increasingly linked to altered gene expression and protein organization. Anchorage dependent cells appear most sensitive to substrate stiffness as they rely on finite resistance to changes in cell generated forces in order to induce outside-in mechanical signals. These signals feed back into cell tension (Wang, et al. 2002), cell adhesion (Choquest, Felsenfeld and Sheetz 1997, Beningo, et al. 2001), posttranslational modification (Beningo, et al. 2001, Pelham and

Wang 1997), protein expression (Cukierman, et al. 2001), cytoskeletal organization (Cukierman, et al. 2001, Engler, et al. 2004a), and cell viability (Wang, Dembo and Wang 2000, A. J. Engler, M. A. Griffin, et al. 2004). If the matrix is rigid, such as glass coverslips, contractile efforts will be isometric. If the matrix is compliant, myocytes will be able to contract in a manner that depends on the stiffness of the substrate itself (Engler, et al. 2004a). The more a cell pulls on its substrate without being able to deform the substrate, the more the cell and its molecules deform rather than the substrate (Engler, Carag-Krieger, et al. 2008). Plating cells onto a glass substrate gives an environment similar to the heart after infarction, the cells will respond in a manner consistent with rigid fibrotic scaring; while on polyacrylamide gels of the optimal stiffness cells will contract as they would in a healthy heart.

Micropatterning:

Mimicking Native Cardiomyocyte Conditions:

In native myocardial tissues, cells are organized into parallel cardiac muscle fibers with contractile myofibrils oriented parallel to the long axis of each cell and intercalated disc complexes concentrated at the ends of each cardiomyocytes in adjoining cells. This delicate architecture is critical for the proper electromechanical coupling of cardiomyocytes to stimulate transmission of a directed contraction over a long distance. In current research, cultured cardiomyocytes will spread and form disorganized myofibrils and diffuse junctions, making it critical to develop a method to address this so that in the future cells represent a native state, or as close to it as possible, when studied. McDevitt, et al., 2001 established a microcontact printing method of laminin to establish

an in vitro system in which spatially defined cues from the substrate guided cardiomyocytes to align and develop normal myocyte architecture. Micropatterned cells formed synchronous beating myofibers that resembled those in native myocardium. In heart tissue, cardiomyocytes connect to one another by intercalated disks which contain N-cadherin and Connexin43. Unpatterned myocytes exhibit connexin43 and N-cadherin around the circumference of the cell, wherever there was contact between cells. This method provides cardiomyocytes with a more effect way for studying extracellular matrix-cell interactions. This patterning technique should allow for cells to potentiate the transmission of cell-to-cell mechanical signals.

Polyacrylamide Gels (PA):

Pelham and Wang established the benefits of growing cells on collagen-coated polyacrylamide gel substrates of varying elasticity. The microenvironment, namely mechanical compliance of the matrix, has become linked to gene expression and protein organization in cardiomyocytes. (Engler, Carag-Krieger, et al. 2008, Pelham and Wang 1997). Actin-myosin striations emerge only on gels with stiffness of normal muscle (Young's modulus E~12kPa). On glass and stiff gels cardiomyocytes from chick explants did not striate.

Cardiomyocytes transmit actomyosin contractions through their attachments to the matrix, if the cells are cultured on glass or rigid gel, the contractile efforts will be isometric. While if on a compliant matrix, cardiomyocytes will contract and generate forces on polyacrylamide gels in direct correlation with the substrate stiffness (A. J. Engler, M. A. Griffin, et al. 2004, Engler, Carag-Krieger, et al. 2008). Embryonic

cardiomyocytes cultured on substrates that mimic the elasticity of the developing myocardial microenvironment are ideal for transmitting contractile work to the matrix and encouraging actomyosin striation. While on hard matrices, similar to a post-infarct fibrotic scar, cells overstrain themselves, lack striated myofibrils and stop beating and on soft matrix cells do very little work (Engler, Carag-Krieger, et al. 2008). On rigid matrices cells are highly strained and cannot significantly strain the matrix, causing myosin based contraction to be fully sustained by the cell, possibly hyperactivating stretch-sensitive proteins, with the end result being inhibition of cell beating. While on a substrate of stiffness ~11-17 kPa, the cell and the matrix are equally strained. Beating of cardiomyocytes is dependent on spreading of the cells and on myofibril reassembly (Engler, Carag-Krieger, et al. 2008, Du, et al. 2003). Cells grown on glass lose their rhythmic contractions, myofibrils and their ability to divide (Engler, Carag-Krieger, et al. 2008, Dabiri, et al. 1999). The ability of cells to reassemble their striations is dependent on substrate elasticity, with few cells on the rigid substrate showing striation and the most striation shown in cells on softer and optimal matrices, 1 and 11 kPa respectively (Engler, Carag-Krieger, et al. 2008). The more an attached cell pulls on its substrate without being able to deform the substrate, the more the cell itself deforms rather than the substrate. Cardiomyocytes from chick explants cultured on glass or stiff PA gels resemble cells after an infarction, with the cells beginning to express myocyte markers, but stopping differentiation before myofibrillogenesis (Shake, et al. 2002).

Development of Model:

As discussed previously, current work on cardiomyocytes is limited to the use of cells on an unpatterned matrix where neonatal rat ventricular myocytes (NRVMs) fail to differentiate and develop an organized sarcomere or on isolated adult cardiomyocytes which lack the ability to form strong extracellular matrix (ECM) adhesions. To overcome these shortcomings, we sought to develop a technique similar to McDevitt et al. 2001 using micropatterning to encourage NRVMs to differentiate into an adult phenotype. This technique allows for NRVMs to maintain their ability to form strong ECM adhesions while differentiating and forming an organized sarcomere and the ability to beat synchronously. These characteristics are necessary to study contractile forces transmitted across the cell membranes and resisted by the ECM, stimulating mechanotranducers and altering cell growth and hypertrophy. Culturing cardiomyocytes on glass coverslips and tissue culture dishes has been a widely accept method for studying these cells in vitro. Recently, Engler et al. 2004 has shown that cardiomyocytes grown on glass substrates have an increase number of stress fibers and begin to deform, while those grown on a flexible polyacrylamide matrix showed little stress and were able to deform their matrix substrate as the cells would in a native state. We sought to bring together the McDevitt patterning technique with Pelham and Wang's cross-linking collagen to PA gels method, much like Engler, et al., 2004 did with myotubes. Cultured patterned neonatal rat ventricular myocytes on PA gels will allow us to measure changes in conractile force and integrin activation in a system mimicking native myocardial tissue. At the same time, we have developed a system mimicking tissue conditions after damage, such as infarction, by patterning ECM onto glass coverslips. The glass coverslip

is representative of post-fibrotic scarring caused by cardiac damage. These two systems allow us to monitor how changes in force generation alter integrin activation in both healthy tissue and scarred tissue.

We hypothesize that mutations and inhibition of sarcomere contractile elements will cause perturbations in traction forces and alter inside-out integrin signaling, initiating a pathological hypertrophic phenotype.

Materials and Methods:

Talin Constructs:

Using whole talin constructs would not be prudent in our work, as we were looking for talin to bind, yet not activate the integrin. Calderwood et al. 1999/2004 showed that the F2F3 and F3 subdomains of talin are able to bind but not activate β1 integrin, yet were capable of activating β3 integrin. We decided to isolate and utilize only the F2F3 and F3 subdomains. Because of this, we could not use a fibronectin matrix, as fibronectin is known to bind β3 integrins. Instead we chose to use laminin as our

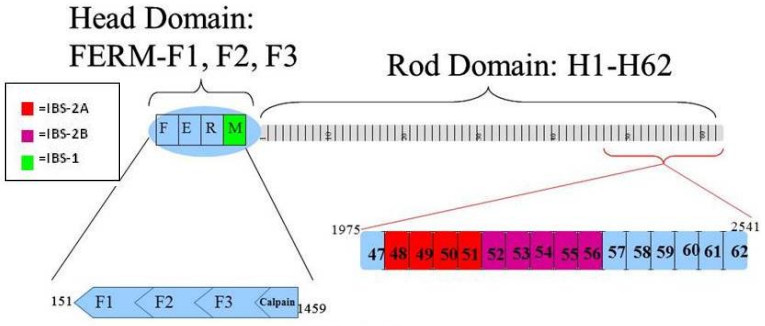

Figure 1: Talin is composed of head and rod domain, both containing an integrin binding site. Talin constructs were selected from recent literature and their known ability to bind yet not activate integrin.

ECM protein as it is known to bind β1 integrins, limiting the possibility of endogenous activation of integrin by our talin construct(s).

RNA Isolation:

FVB mice were obtained from core Animal facility at University of Nevada, Reno and humanely euthanized using CO2 followed by cervical dislocation. The liver, spleen, kidney, and brain were dissected from the mice and placed immediately into RNAlater to preserve RNA and flash frozen in liquid nitrogen before being stored at -80 ℃. Qiagen RNeasy midi kit and protocol was used to isolate RNA from tissues. Briefly, tissues were homogenized in the appropriate buffer and the lysate was centrifuged and the supernatant was removed and used subsequently. 70% Ethanol was added to the supernatant before being applied to an RNeasy Midi column and centrifuged. Subsequent steps purified, washed, and eluted the RNA from the column for future use.

cDNA Synthesis:

RNA was used to synthesize cDNA using SuperScript III Reverse Transcriptase (Invitrogen). Briefly, 2pmol gene-specific reverse primer was mixed with 2ug RNA, 10mM dNTPs, and distilled water; the mixture was heated for 5 minutes at 65 ℃ and then incubated on ice for 1 minute. 5X First-Strand Buffer, 0.1M DTT, RNaseOUT, and SuperScript III Reverse Transcriptase were added to the mixture and incubated at room temperature for 5 minutes. The mixture was then incubated at 55 ℃ for 1 hour and then inactivated at 70 ℃ for 15 minutes.

Amplification of Talin Constructs:

cDNA was then used as a template for PCR amplification using talin gene-specific primers. Primers encoding talin head regions; 151-177, 457-480, and 829-847 with one of two reverse primers 1252-1231 or 1459-1435, were used to amplify cDNA constructs using standard PCR conditions and Taq DNA Polymerase (Promega). Amplified samples were ligated into pcDNA3.1/CT-GFP-TOPO (Invitrogen) and then transformed into One Shot TOP10 chemically competent E.Coli cells. (Invitrogen) Transformation reactions were then spread onto LB-Ampicillin plates and colonies were screened using PCR and restriction digest. Positive colonies were grown in small scale preps for sequencing. Samples with correct sequence orientation were then grown into large scale preps for future experiments.

Transfection of C2C12 Cells:

C2C12 cells were cultured to ~70% confluence and then transfected with talin DNA samples using TransIT-LT1 transfection reagent (Mirus Bio, Madison, WI). Briefly, cells were cultured in 4-well chambered coverglass plates (3×10^5 cells/well) and allowed to culture overnight. TransIT-LT1 reagent was warmed to room temperature and vortexed before use. 26 µl Opti-MEM (Invitrogen) was placed into a 1.5ml eppendorf tube. 0.79 µl TransIT-LT1 reagent was added and mixed using a pipette. 0.5-1 µg talin DNA was added to the diluted TransIT-LT1 reagent. Solution was mixed gently and allowed to sit at room temperature for 30 minutes. Mixture was added dropwise to the cells with gentle rocking to evenly distribute the reagent-DNA complex

evenly. Cells were monitored for green fluorescence and later fixed and stained using GFP and α5 integrin antibodies and imaged using confocal microscopy.

Immunofluorescence:

Media was first removed and cells were rinsed briefly with sterile 1XPBS before being fixed with 3.7% formaldehyde for 10 minutes. Formaldehyde was removed and cells were rinsed again, cells were permeabilized with 0.3% Triton-X for 5 minutes and again rinsed. Cells were blocked with 2% BSA for 1 hour. Primary antibodies were diluted in 2% BSA + 0.1% Tween-20 overnight at 4 ℃. The following day primary antibodies were removed and cells were rinsed with 1X PBS + 0.1% Tween-20, four times five minutes each. Secondary antibodies were diluted in 1% BSA + 0.1% Tween-20 and incubated at room temperature for one hour. Secondary antibodies were removed and cells rinsed with 1X PBS +0.1% Tween-20, 4 times five minutes each and then rinsed with 1X sterile PBS, 4 times five minutes each. Cells were stored in sterile PBS at 4 ℃.

Adenovirus Construction:

pShuttle-CMV (Agilent Technologies) contains a multiple cloning site between a CMV promoter and an SV40 polyadenylation signal and is able to accommodate the insertion of large DNA.

Cloning the Gene of Interest: Talin DNA was excised from pcDNA3.1-CT/GFP using PCR and subsequent restriction digest and cloned into pShuttle-CMV multiple cloning site between restriction sites KpnI and HpaI. Shuttle vector DNA containing talin was purified and linearized using PmeI and complete digestion was confirmed using

agarose gel electrophoresis. Linearized DNA was transformed into BJ5183-AD-1 (Stratagene). Briefly, BJ5183-AD-1 cells were thawed and 40µl placed into a chilled microcentrifuge tube. 0.1µg of linearized shuttle vector was added to the cells and the solution was transferred into a chilled electroporation cuvette which was then placed into an electroporation chamber with the electroporator set at 200Ω, 2.5kV, and 25µF. The samples were pulsed and then removed quickly from the electroporator and 1ml of sterile LB broth was added. The cell solution was transferred to a 14ml BD Falcon polypropylene round-bottom tube. The cells were incubated at 37 ℃ for 1 hour with shaking at 225-250rpm. Transformed cells were then plated onto LB-[25 µg/ml] kanamycin agar plates and incubated over night at 37 ℃. Recombinants were screened using PacI enzyme and positives were identified by dropping either a 3.0 or a 4.5 kb band. Positive recombinants were transformed into Chemically Competent TOP10 cells and a large scale prep was prepared. Approximately 5µg of DNA was digested with PacI enzyme and prepared for transfection into AD-293 cells.

Transfecting AD-293 Cells: HEK-293 cells were ensured to be 70% confluent before transfection. Serum free media was prepared and added to the plated cells 30 minutes before transfection. PacI digested DNA was added to a 5ml BD Falcon polystyrene round bottom tube containing sterile water to a final volume of 225µl. 25µl Solution I (2.5M $CaCl_2$) and 250µl Solution II (2X BBS) was added to the tube and incubated at room temperature for 10 minutes. The mixture was added to the plates dropwise with swirling to ensure proper dispersion. Cells were incubated at 37 ℃ for 3 hours and media removed and replenished. Cells were allowed to culture for 7-10 days with media being replenished as needed (according to pH color indicator).

Preparing Primary Viral Stocks: Growth media was removed from the adenovirus producing HEK-293 cells and the cells washed with PBS. 0.5ml PBS was added to each plate needing to be harvested and cells were collected by carefully scraping the cells into the pool of PBS. The PBS containing cells was transferred to a microcentrifuge tube and the sample(s) were subjected to four rounds of freeze/thaw by alternating tubes between a dry ice-ethanol bath and a 37 ℃ water bath. Cellular debris were collected by microcenrifugation at 12,000X g for 10 minutes at room temperature. The supernatant was transferred to a fresh microcentrifuge tube and stored at -80 ℃.

Purification of Virus: Following Adeno-X Maxi Purification Kit User Manual. Briefly, five 150mm plates with HEK-293 cells were infected with 50 µl F2F3 adenovirus, viral titer had not yet been determined. Cells were incubated at 37 ℃ and 5% CO_2 until cytopathic effect is complete. Infected cells were pelleted by centrifugation at 1500 rpm for 10 minutes, supernatant was discarded and pellet resuspended in fresh medium. Cells were lysed with three consecutive freeze-thaw cycles and centrifuged again after the final thaw at 3000rpm for 5 minutes. Supernatant was saved and pellet discarded. 5µl Benzonase Nuclease was added to the supernatant and incubated for 30 minutes at 37 ℃. Sample was diluted with an equal volume of 1X Dilution buffer and the lysate filtered through a 0.45µm syringe-tip pre-filter using the 20ml syringe that is provided in the kit. The filter assembly was equilibrated with 5ml 1X Equilibration Buffer. Lysate was loaded onto the purification filter by pushing the lysate through the filter, allowing the virus to bind. 20 ml 1X Wash Buffer was pushed through the filter. 1 ml of Elution Buffer was pushed through the filter and collected in a 15 ml conical tube. The filter was incubated at room temperature for 5 minutes before an additional 2 ml of

elution buffer was pushed through the filter and collected in the 15 ml conical. Virus was aliquoted and stored at -80 ℃.

Determining Viral Titer: HEK-293 cells were seeded at $2.5X10^5$ per well in a 24 well plate. Virus was prepared in 10 fold dilutions and 100 µl of each viral dilution was added to each well in duplicate. Cells were incubated at 37 ℃ and 5%CO_2 for 48 hours. Media was removed and cells dried in the hood before cells were fixed with 1 ml ice cold 100% methanol. Cells were incubated with methanol at -20 ℃ for 10 minutes. Methanol was removed and cells rinsed with 1 ml 1X PBS + 1% BSA. 0.5 ml Mouse-anti-Hexon antibody (1:1000 in PBS + 1% BSA) dilution was added to each well and incubated at 37 ℃ for 1 hour. Antibody was removed and cells rinsed 3 times with PBS + 1% BSA. 0.5ml Rat-anti-Mouse antibody (1:500 in PBS + 1% BSA) was added to each well and incubated again at 37 ℃ for 1 hour. Cells were rinsed with PBS + 1% BSA and 250 µl 1X DAB solution was added to each well and incubated at room temperature for 10 minutes. DAB was removed and 1ml PBS added. Cells were imaged under light microscopy and brown/black cells were counted. The infectious units/ml was calculated to be $4.07X10^8$ infectious units/ml.

Preparing Stamp:

Wafer (Fig. 2) was placed on molding and secured in place with parafilm. A solution of silicone : curing agent was mixed at a 10:1 ratio (80ml silicone to 8ml curing agent). Mold was filled 2/3 full to prevent overflow and placed in dessicator.

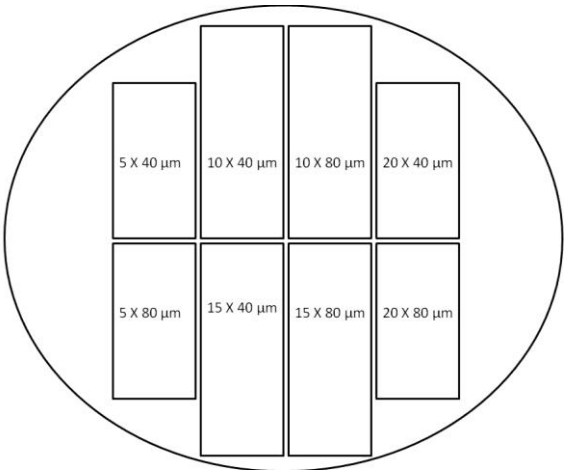

Figure 2: Burn pattern of our custom made mold allowed us to explore which measurements led to the best spacing between lanes and width of the lane itself.

Stamp was allowed to cure for more than 1 hour at a pressure of 20inch Hg.

Conjugation of Laminin to Oregon Green-488:

0.5 mg of Oregon Green-488 (Molecular Probes, Eugene, OR) was dissolved in 50 µl of DMF and added to 2mg of laminin in PBS. The solution was shielded from light and incubated overnight at 4 ℃ with rotation. Solution was aliquoted and stored at -80 ℃; 5 µl labeled laminin was mixed with unlabeled laminin to a final concentration of 45 µg/ml.

Stamping:

Stamps were cut and submerged in 70% ethanol for 1 hour and then rinsed with distilled water three times before use and placed in sterile petri dishes in the culture hood patterned side up. Stamps were air dried under UV for 30 minutes; the patterned sides of the stamps were then covered with 45µg/ml labeled or unlabeled laminin (Invitrogen) for 1 hour at room temperature (laminin-stamp incubation phase). Excess laminin was removed from the surface and then rinsed with water, and dried. Stamps were then placed patterned side down on glass or polyacrylamide gel for 1 hour or overnight, corresponding to the substrate, at 37 ℃ (stamp-substrate phase). Stamps were removed and stamped plates were stored at 37 ℃ until further use. Before use plates were blocked for at least 1 hour with 1% BSA at 37 ℃.

Stamping Optimization-Temperature: Stamps were incubated at 37 ℃ during both the initial laminin-stamp incubation phase and during stamp-substrate contact phase (Fig. 3). Stamps were then incubated at 37 ℃ during either the laminin-stamp phase or the stamp-substrate phase. Stamped plates were then stored at either 4 ℃ or 37 ℃ to determine which set of temperature combinations yielded the most consistent patterning.

Stamping Optimization-Concentration: Laminin stock 1mg/ml was diluted with PBS to a final concentration ranging from 45-100μg/ml and optimal concentration determined through a set of titration experiments, where laminin dilutions were stamped onto substrate and imaged using confocal microscopy to determine which yielded optimal patterning without crystallization or low laminin transfer efficiency.

Stamping Optimization-BSA Blocking: 1% BSA was first added to glass plates before stamping was carried out. Alternatively, plates were first stamped and then blocked with 1% BSA for 1 hour before plating NRVMs. Cell patterning was compared between the two by imaging with basic light microscopy to determine extent of cell

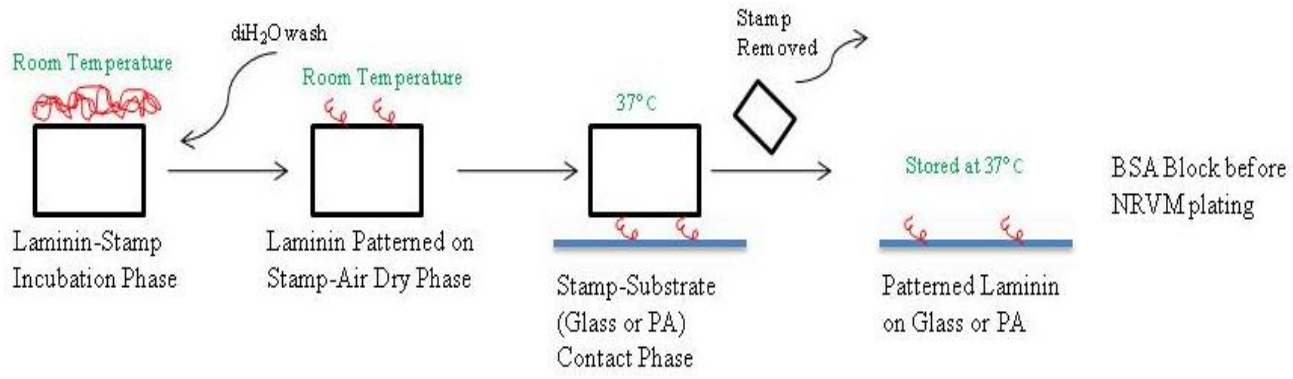

Figure 3: Stamping overview. Laminin is incubated on the stamp at room temperature for 1 hour. Excess laminin is then removed and the stamp rinsed with water and dried. Stamp is placed patterned side down on desired substrate for a time ranging from 1-24 hours. Stamp is removed and plates are incubated at 37 ℃ until use.

Laminin-Coated Polyacrylamide Gels:

Adapted from Wang and Pelham 1998.

Preparation of Glass Coverslips: Coverslips were passed through a flame before smearing a small amount of 0.1N NaOH across the surface of the slip and were allowed to air dry into a film. Approximately 200µl of 3-aminopropyltrimethoxysilane (3-APMS) was applied evenly onto the NaOH treated surface and allowed to sit for 5 minutes. Coverslips were then covered with distilled water and allowed to sit an additional 5 minutes until glass appeared clear again; coverslips were then rinsed with water with rotation for 10 additional minutes. The treated surface was then covered with 0.5% glutaraldehyde in PBS and incubated at room temperature for 30 minutes.

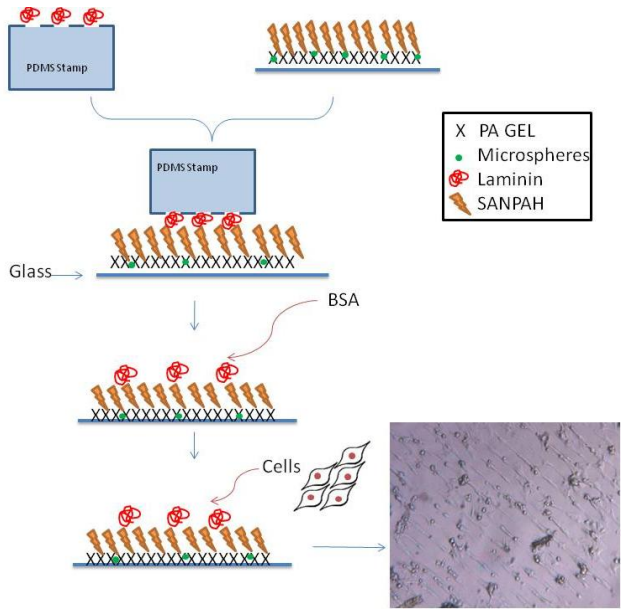

Figure 4: Overview of stamping method on polyacrylamide gels. Laminin is incubated on stamp and stamping carried out as shown in Fig. 2. Polyacrylamide gel surface is cross-linked to laminin using SANPAH. Gels are prepared the day before cell isolation to ensure SANPAH does not breakdown. Gels are BSA blocked for 1 hour before cells are plated.

Preparation of Polyacrylamide Gels:

To obtain varied elasticity, the amount of cross linker, bis-acrylamide, is adjusted. Acrylamide, N,N'-Methlene bisacrylamide (BIS), and water were mixed to the desired concentration, 10%Acrylamide: 0.3%BIS. For gels containing beads: beads were sonicated briefly before being added to the acrylamide mixture at a ratio of 1/125. The

solution was degassed before the addition of 10% ammonium persulfate (APS) at a volume ratio of 1/200 and N,N,N',N'-tetramethlethlenediamine (TEMED) at a volume ratio of 1/2000. 10-25ul of the solution was added to the activated surface of the coverslip (varied according to desired gel thickness) and covered with another coverslip. The assembly was turned upside down to allow the beads to settle onto the surface of the gel; in the event no beads were added the assembly was allowed to sit without turning upside down. The gel was allowed to polymerize for 30 minutes. After polymerization the top coverslip was carefully removed and the gel washed with 50mM HEPES (pH 8.5).

Activation of the Polyacrylamide Surface: 200µl of 1mM sulfo-SANPAH was applied to the surface of the gel. The surface was exposed to UV light of a 15W germicidal lamp at a distance of 3 inches for 5 minutes. Darkened sulfo-SANPAH solution was removed and the UV exposure repeated. The gel was then washed with 50mM HEPES for 15 minutes with agitation twice. Stamping was performed as discussed previously with the stamp remaining in contact with the gel overnight at 37℃. The following morning stamps were carefully removed and the gels blocked with 1%BSA for 1 hour at 37℃ before plating cells onto the now patterned gels (Fig. 4).

Buffers and Medias:

10X ADS: 6.8g of NaCl (1.1M), 4.76g HEPES (0.2M), 0.12g NaH_2PO_4 (0.01M), 1g Glucose (0.05M), 0.4g KCl (0.05M), and 0.1g $MgSO_4$ (0.01M) were combined into 90ml dH_2O. The pH was adjusted to 7.35 (+/- 0.5) before bring to final volume of 100ml with dH_2O. The solution was filter sterilized with 0.22µM filter and stored in a sterile bottle at 4℃.

Percoll Gradient: Percoll stock was mixed at a ratio of 9 part percoll: 1 part 10X ADS Stock. Two buffers of different densities are used in the Percoll gradient; the top buffer is composed of 4.5ml Percoll Stock + 5.5ml 1X ADS yielding a density of 1.059. The bottom buffer is composed of 6.5 ml Percoll Stock + 3.5ml 1X ADS yielding a density of 1.082. To make the percoll gradient, 4ml of top buffer was placed into a 15ml conical tube, 3 ml of bottom buffer was underlayed, and if done correctly a sharp interface will be present.

Cardiomyocyte Media: In a large 1000ml beaker, 50ml of heat-inactivated horse serum, 25ml of heat-inactivated fetal bovine serum, 2g HEPES (15mM), 105ml M199 media, and 315ml DMEM High Glucose were combined and mixed thoroughly. The pH was then adjusted to 7.3 and 5ml of penicillin/streptomyocin was added before the entire solution was filter sterilized and stored in a sterile container at 4 ℃.

+BRDU: BRDU was added to cardiomyocyte media just before use in cell culture at a final concentration of 25μM.

Serum-Free Cardiomyocyte Media for Infection of NRVMs: Media is prepared as cardiomyocyte media is, without fetal bovine serum and horse serum. ITS was added just before infection into NRVMs at a ratio of 1ml ITS per 100 ml media.

Isolation of Neonatal Rat Ventricular Myocytes (NRVMs):

3 day old rat pups were sprayed with 70% Ethanol prior to decapitation. Hearts were dissected out and placed into a 50ml conical tube containing ~5ml 1XADS buffer. Hearts were rinsed with buffer to release blood clots and extracardiac tissue; the supernatant was discarded and the hearts poured into a sterile petri dish on ice. Atria and

excess tissue were removed from the ventricles. Hearts were then minced and placed into a 50ml conical tube containing ~5ml 1XADS + [25ug/ml] Liberase Blenzyme (Roche). Cells were incubated with rotation for 10 minutes at 37 ℃; the initial supernatant was discarded and fresh digestion buffer was added to the cells. Following 10 minute digestion the supernatant was pipetted into a 50ml conical containing 15ml cardiomyocyte media. Digestion process was repeated until all tissue was gone. Cells were pelleted at 1000rpm (Thermo IEC cenraCL2 centrifuge) for 5 minutes. The supernatant was discarded and cells were thoroughly resuspended in 4ml of cardiomyocyte media, 2ml of cells were added to each of two percoll gradients. Percoll gradients were then spun at 2060rpm for 30 minutes (GH-38 Rotor). Ideally two bands of cells will be visible, the top layer containing fibroblasts and the lower band containing myocytes. Collected cardiomyocyte containing bands and transferred bands to a new 50ml conical tube, diluted with an equal volume of media, and centrifuged for 5 minutes at 1000rpm. The supernatant was discarded and cells were resuspended in 10ml of media before counting on the hemocytometer. We plated cells at our desired concentration and replaced the growth medium approximately 6 hours after initial plating. Media was changed daily, with half the media being replaced. NRVMs were plated at a density of 250,000 cells per 1.54cm^2.

Infection of NRVMs with F2F3 Adenovirus:

NRVMs were allowed to differentiate for 3 days before infection with F2F3 adenovirus. Serum-containing media was removed and replaced with serum-free cardiomyocyte media + ITS. Virus was added at an MOI of 1 or 5 (0.614 µl or 3.07 µl

respectively). Virus was kept on cells for 6 hours and then media containing virus was removed from cells and replaced with fresh serum-free media. Cells were monitored for expression of GFP and then imaged using TIRF microscopy.

*TIRF Microscopy**:***

NRVMs were loaded onto cell culture imaging chamber RC-21BRFS (Warner Instruments) and fitted onto the PM Series Chamber Platform PM-2 (Warner). Cells were then imaged using Nikon Eclipse TE 2000-U and videos were captured in Simple PCI at 0.05 seconds/frame. Video images were converted to TIF files and analyzed using ImageJ software where regions of interest were selected and the change in intensity over time was analyzed and measured. ImageJ results were uploaded into Microsoft Excel to generate a plot of intensity change vs. time.

Results:

Glass Stamping:

Optimization: Lane Width-Distance between lanes:

We first had to recreate and optimize the methods described by McDeviit et al 2001. Photomask was ordered from Microchem and contained the dimensions seen in Fig. 2 allowing us to independently verify the optimal lane length and distance between lines. We found that 10X80 stamps yielded individual cardiomyocytes patterned with little to no bridging across the lanes Fig 5. G.

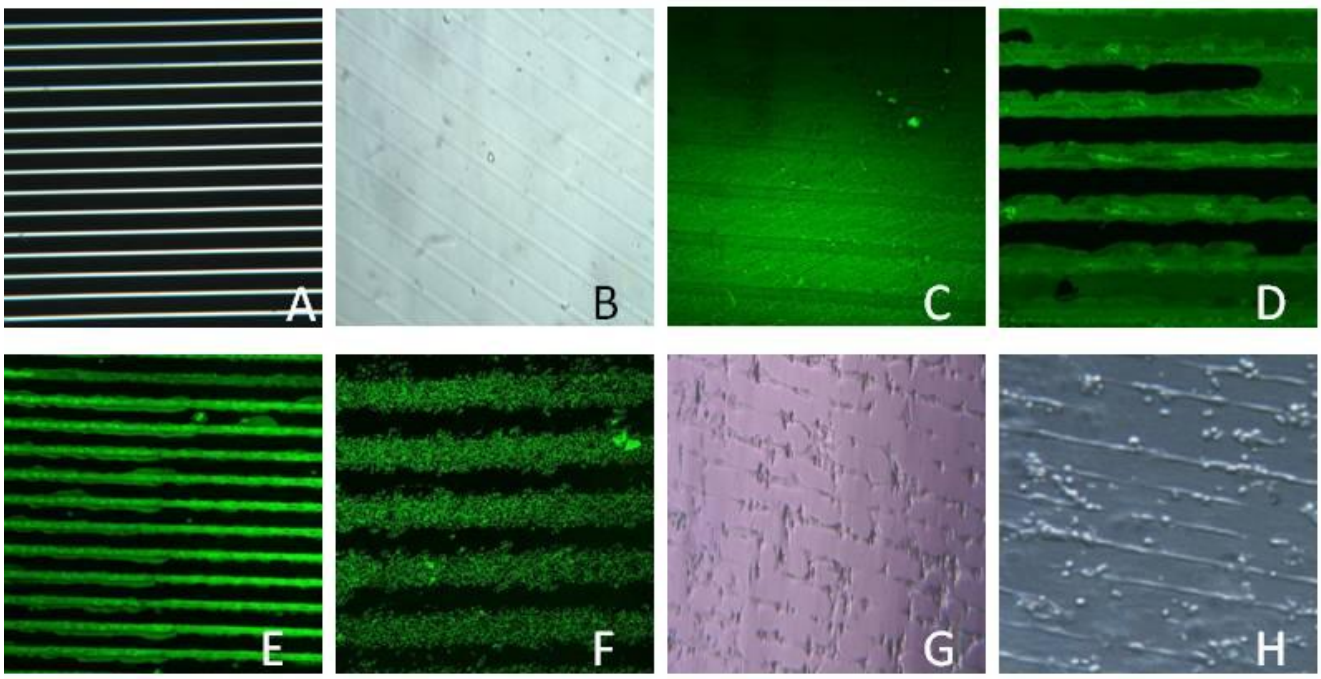

Figure 5: A) Photomask depicting lane spacing used to create mold. B) PDMS stamp made from mold showing distinct lanes and valleys. C) Labeled laminin stamped at concentration of 100µg/ml D) Labeled laminin incubated at 37℃ during initial laminin-stamp phase and stamp-glass phase. E) 45µg/ml laminin incubated at 37°C during stamp-glass phase only. F) Patterned laminin mixed with microspheres. G) Patterned NRVMs on glass H) Patterned NRVMS on polyacrylamide gel

Optimization: Temperature, Laminin Concentration, BSA Blocking

To optimize our technique and increase reproducibility, laminin was conjugated to Oregon Green 488 (Molecular Probes), enabling us to visualize successful pattern transfer Fig. 5E.

Laminin Concentration: We sought to determine the optimal amount of extracellular matrix protein to adhere cells to the plate in designated lanes, while not inhibiting contraction and maintaining cell adherence during future pacing experiments. Laminin concentrations were varied from 45-100μg/mL. We found that increasing the concentration to 100 μg/mL led to laminin sheets Fig. 5C across the plate. Systematically reducing the concentration of laminin to an optimal 45 μg/mL showed laminin lines of optimal thickness and patterning with no bridging (Fig. 5G).

Temperature: From the literature, we knew that laminin forms polymers at 35 ℃ and breaks down into monomers at 4 ℃, therefore we initially incubated laminin on the stamps at 37 ℃ followed by incubating the stamp at 37 ℃ during the stamp-substrate contact phase. This caused the formation of huge laminin crystals and sheets of laminin bridging across the lanes (Fig. 5D). We found that incubating the stamps with laminin at room temperature followed by incubation during their substrate contact phase with glass at 37 ℃ yielded optimal laminin transfer (Fig. 5E). Stamped plates were then stored at 37 ℃ to maintain laminin polymers and prevent breakdown back to monomers.

BSA Blocking: Blocking with BSA had been done before stamping previously and yielded low reproducibility and efficiency with stamping. We sought to determine if

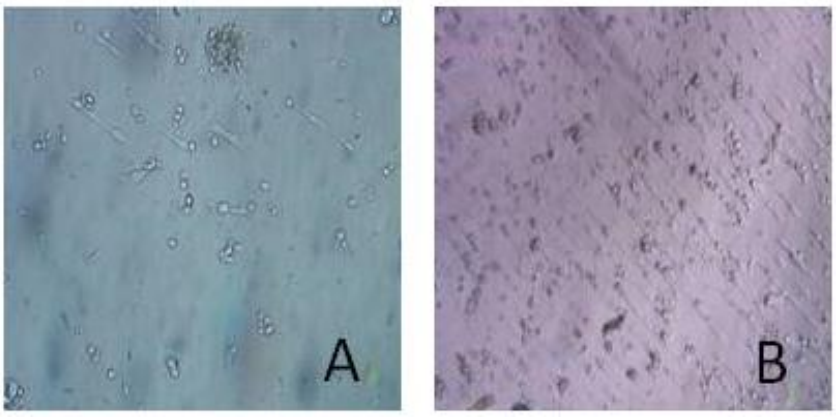

Figure 6: A) BSA Blocking before stamping B) BSA blocking after stamping

blocking with 1X BSA after stamping led to increased laminin transfer and increased reproducibility. We found that stamping laminin followed by blocking with 1%BSA one hour before plating cells yielded consistent patterning. (Fig. 6 A & B)

Cardiofilament Formation on Glass:

We were successful in optimizing our stamping technique which can be seen from start to finish in Fig. 5. Patterned NRVMs were stained to confirm the presence of intercalated discs and α-actinin, at 3, 5, and 7 days (Fig. 7 D-F), which would indicate the development of organized sarcomere. We can see that by day 5-7 NRVMs begin to deteriorate and produces excess connexin-43. The optimal day for these cells was around Day 3, where they show a healthy sarcomere and have not begun to deteriorate, limiting

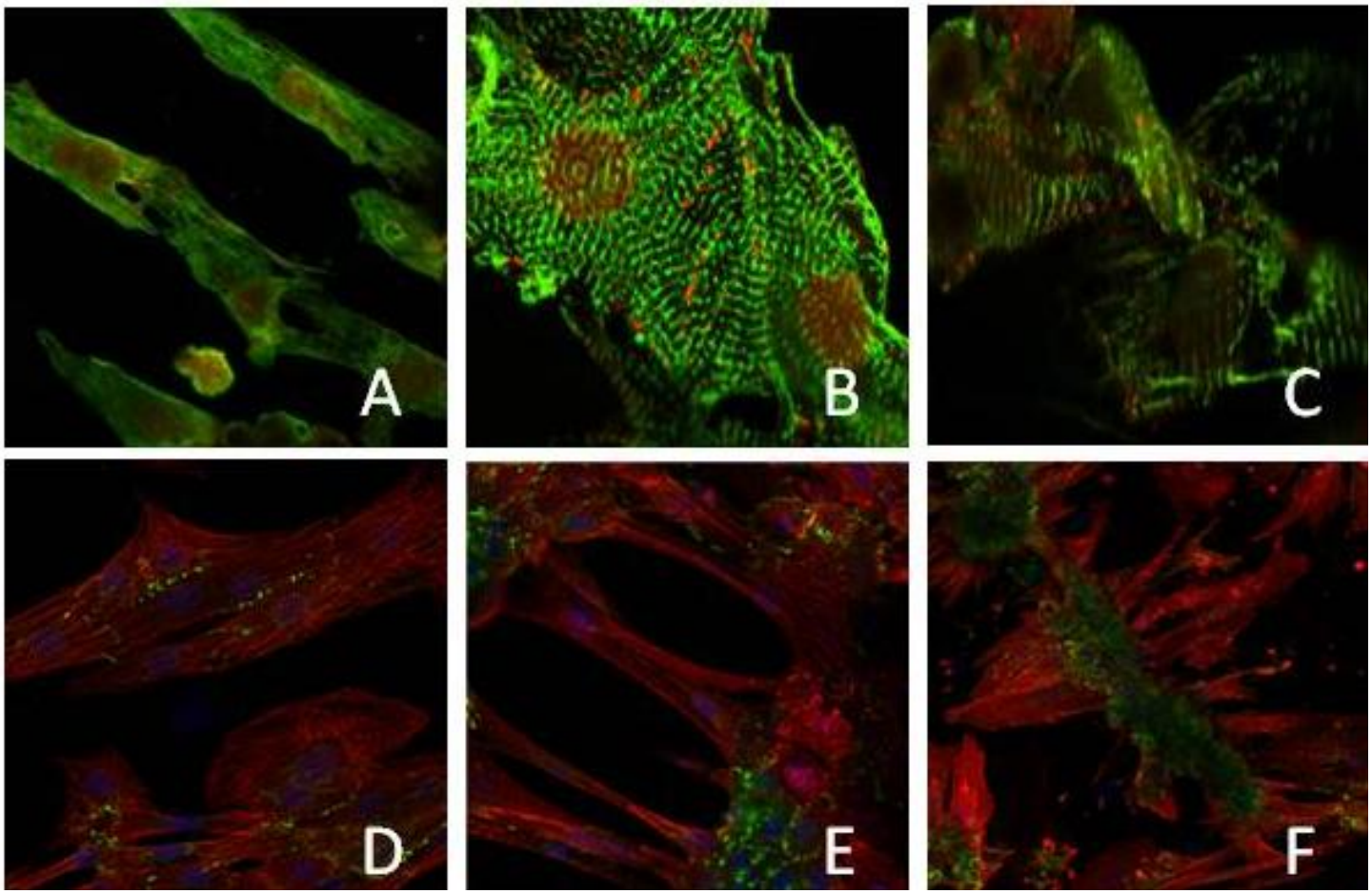

Figure 7: Patterned cardiofilaments on polyacrylamide gel (top) or on glass (bottom). A-C) NRVMs patterned on flexible polyacrylamide gel stained with connexin-43 (red) and α-actinin (green) at 3,5,7 days, respectively. D-F) NRVMs patterned on glass substrate stained with connexin-43 (green) and α-actinin (red) at 3,5, 7 days, respectively.

the number of experiments we could do.

Polyacrylamide Gels:

We designed a method that combines the technologies developed by McDevitt

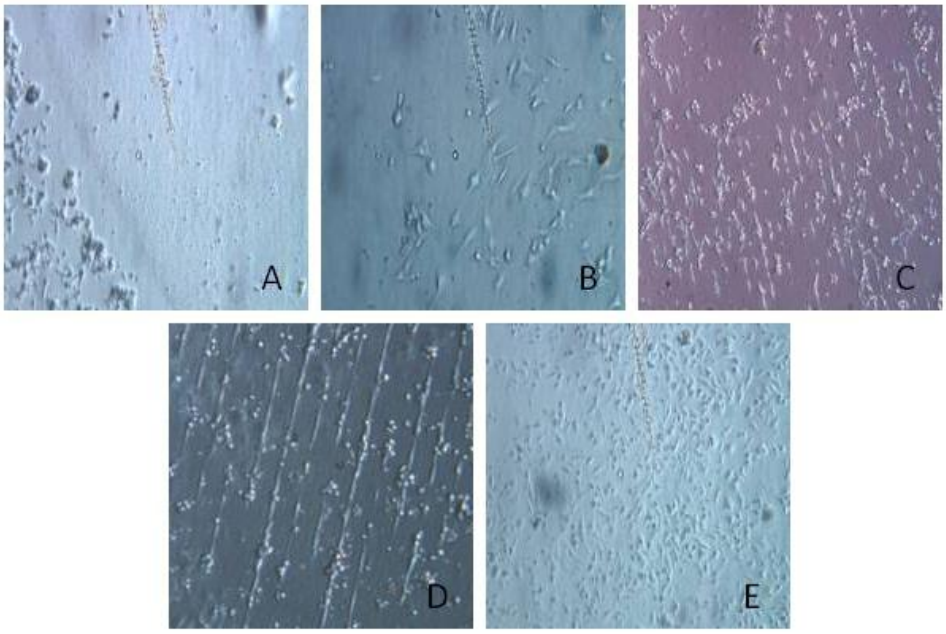

Figure 8: Stamp-polyacrylamide gel contact phase optimization. A) 1 hour contact phase B) 3 hours C) 6 hours D) Overnight E) Laminin control

2001 and Pelham and Wang 1998 method for patterning polyacrylamide gels. We are still optimizing this technique, but we have obtained promising results thus far. We were able to successfully stamp and obtain patterned cells on the PA surface (Fig. 8D).

Optimization Time of Stamp-Polyacrylamide Gel Contact: We found that allowing the stamp-PA gel contact phase to proceed for only one hour as we had on glass did not yield patterning. (Fig . 8B). PA gels were stamped for 0, 1, 3, 6, and 12 hours (Fig. 8A-D). Six hour incubation contained some patterning which looked similar to what we had seen on glass. Stamping overnight (Fig. 8C) led to the most consistent patterning and yielded the longest cardiofilaments we had seen to date (Fig. 8D).

Formation of Cardiofilaments on PA Gels: When patterned NRVMs were stained at 3, 5, and 7 days we did not see the same deterioration as we saw on glass (Fig. 7A-C). In contrast, Day 3 (Fig. 7A) showed very little sarcomere development, while at day 5 (Fig. 7B) and beyond we had healthy sarcomere formation and intercalated discs. Cardiomyocytes plated on PA gels were contractile within 12-24 hours and maintained contraction for >20days (longest observed).

Beads Embedded in PA Gels vs. Beads Mixed with Laminin: To measure contractile force, we aimed to utilize a method measuring bead displacement in the matrix. Initially, we mixed laminin with fluorescent microspheres and stamped onto glass coverslips and successfully got laminin transfer. (Fig. 5F). Upon plating cells we stained the cell nuclei with bis-benzamide and imaged cells under confocal microscopy. Microspheres fluoresce under all wave lengths (Fig. 9D), while the nuclei fluoresced under 405nm (Fig. 9C). Patterned NRVMs and beads, but NRVMs appeared to absorb the beads into their matrix, which could disrupt future displacement measurements and lead to inaccuracies. As we moved forward with polyacrylamide gels, we were able to add microspheres to the PA gel itself (Fig. 9A) and saw that cells did not absorb the beads as seen on glass (Fig. 9B).

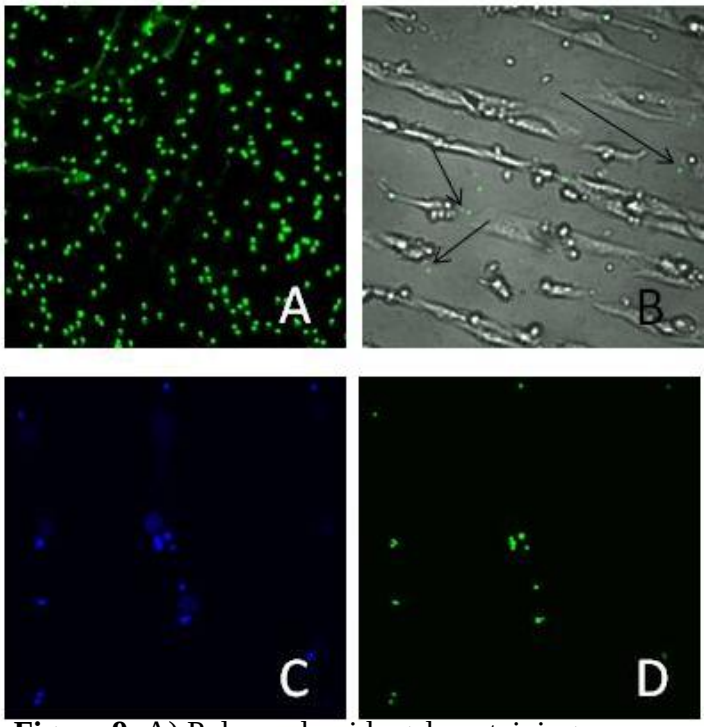

Figure 9: A) Polyacrylamide gel containing fluorescent microspheres B) Patterned NRVMs on PA gel embedded with fluorescent microspheres. C) NRVMs on patterned laminin matrix embedded with microspheres, nuclei (blue) D) Patterned laminin with microspheres from image C at 488nm.

Amplification of Talin DNA:

RNA isolated from liver of FVB (Friend Leukemia Virus B Strain) mice was successfully transcribed with oligonucleotides to create cDNA, which was then to amplify our DNA constructs using gene specific primers coding for the talin head domains: Full Talin Head, F2F3, and F3 domains, and for the rod domains: H48-62, H50-58, H50-62 (Fig. 10).

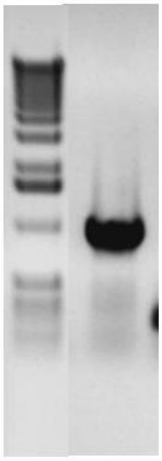

Figure 10: Amplification of F2F3 construct from FVB liver cDNA showing band at ~773kb.

Our initial goal was to have multiple samples to infect cells with. Constructs were then transiently transfected into C2C12 cells to determine their ability to localize with integrin at focal adhesions (Fig. 11). From there cells were stained with for integrin (Fig. 11B & E, red), GFP (Fig. 11 C & F, green), and nuclei stain (blue) and imaged using confocal microscopy. We found that the full talin head, F2F3, and F3 domains were colocalized with talin at focal adhesions (A-C and D-F), while the talin rod domains did not (Data not shown). These 3 positive samples were then digested out of the PCDNA 3.1 CT/GFP-TOPO vector and ligated into pShuttle-CMV vector. The FTH and F3 domains had to be abandoned due to difficulty ligating into the shuttle vector, thus from here we moved

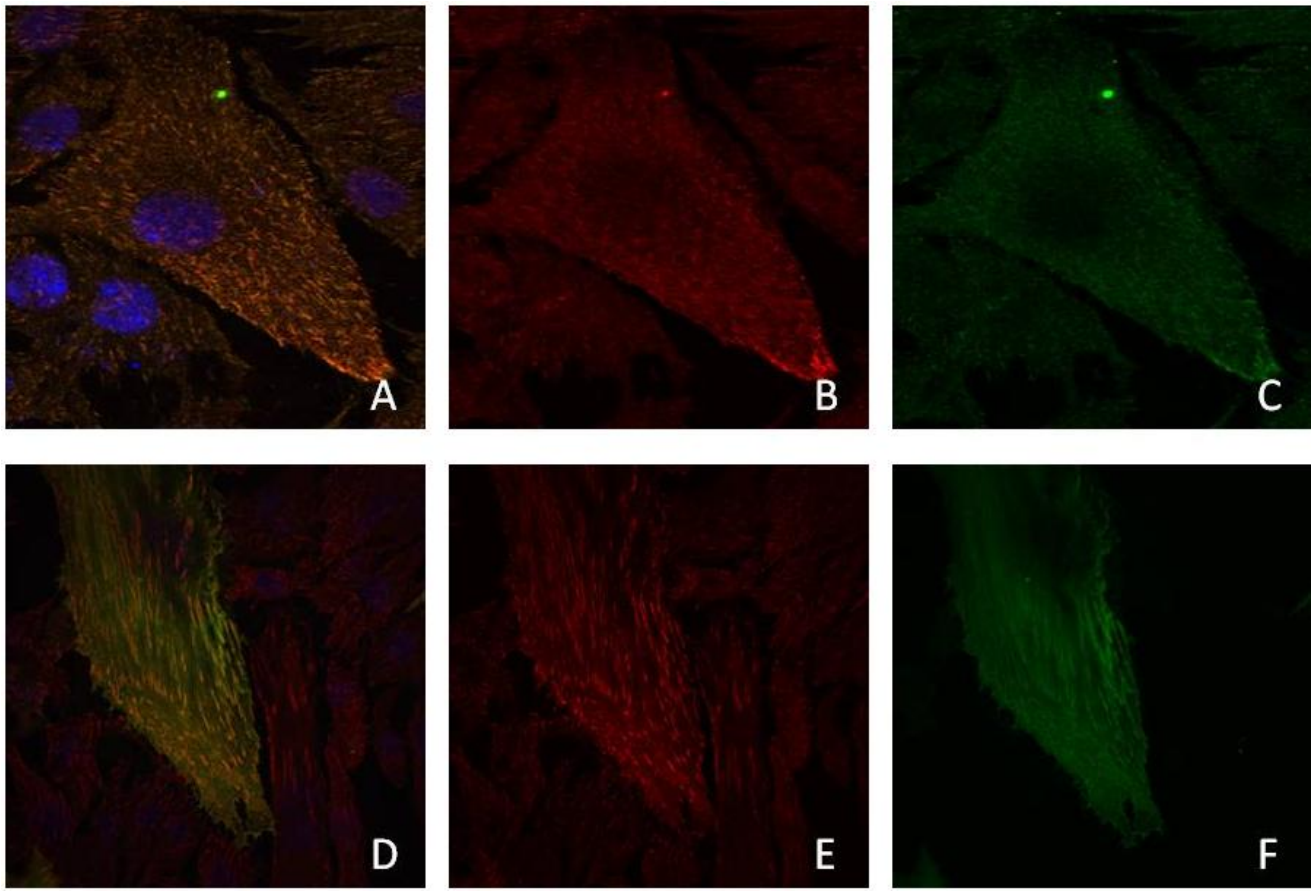

Figure 11: C2C12 cells transfected with F2F3 (top) or FTH (bottom). A & D) overlay, B & E) Integrin, C & F) GFP

forward with the F2F3 domain only.

pShuttle-CMV containing F2F3 subdomains was then recombined with the AdEasy virus backbone to become the adenovirus (Fig. 12). Virus was amplified, purified, and tittered.

Infection of NRVMs with F2F3 Adenovirus: Cardiomyocytes were infected at MOI of 1, 5, 10, and 20 to determine optimal MOI. An MOI of 5 yields the most consistent infections without killing the cells. Cells were stained and imaged using confocal microscopy to once again determine the construct's ability to localize with integrin at focal adhesions (Fig. 13).

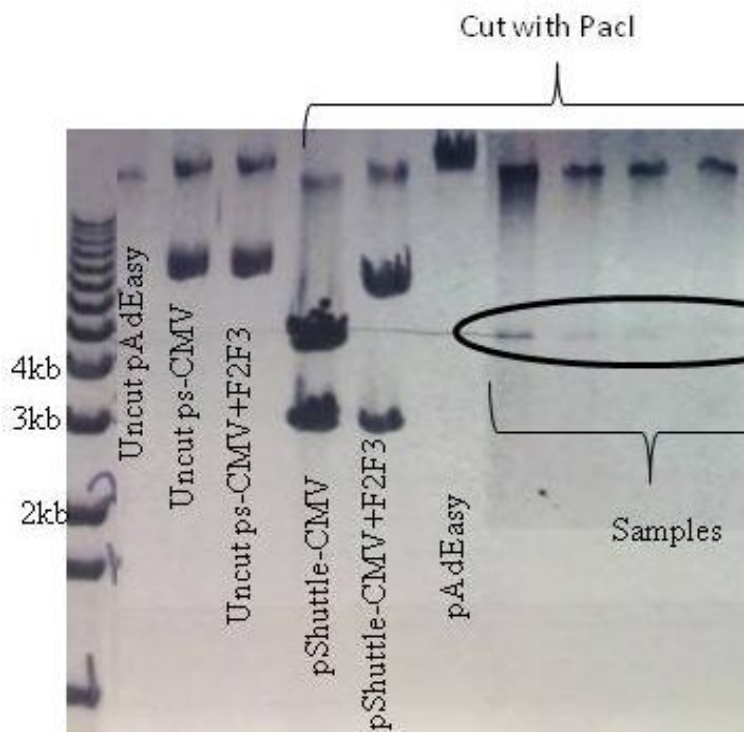

Figure 12: Positive F2F3 recombinant adenovirus. Positive recombinants dropped a band at either 3.5 or 4 kb after digestion with PacI enzyme.

Separate infected cells were then imaged using widefield microscopy to visualize these FA's in real time (Fig. 14). Fig 15 shows that we can clearly visualize successful infection of F2F3-GFP virus and possible FAs in cardiomyocytes.

Cells showed clear focal adhesions, which was confirmed through confocal microscopy (Fig. 13) where we can clearly see talin-GFP colocalizing with integrin. This was also confirmed through real-time widefield microscopy (Fig. 14), where focal adhesions appeared as punctuate dots.

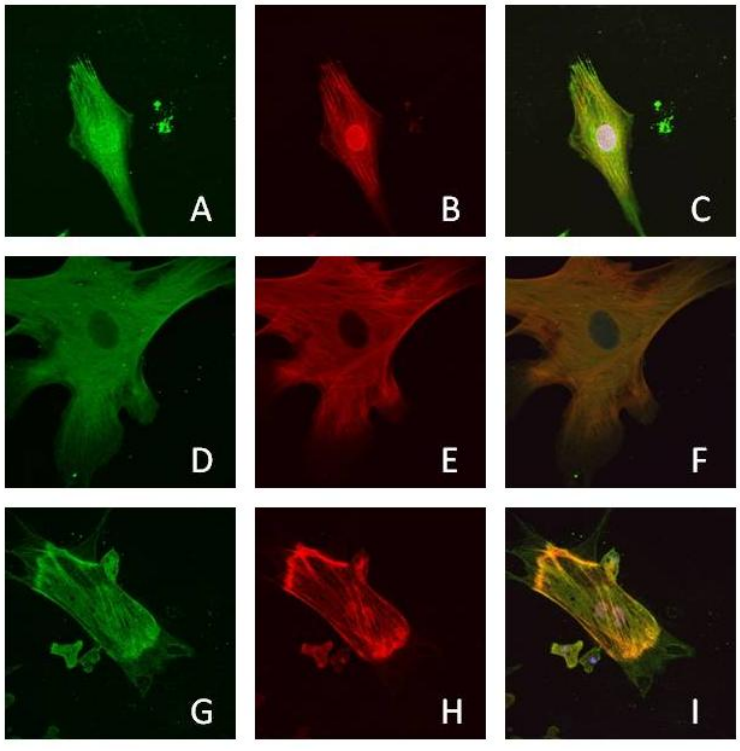

Figure 13: Infected NRVMs plated on PA gels and stained for β1 integrin (red), talin GFP (green), and overlay. A-C) MOI 1 D-I) MOI 5 K)Uninfected Control NRVM

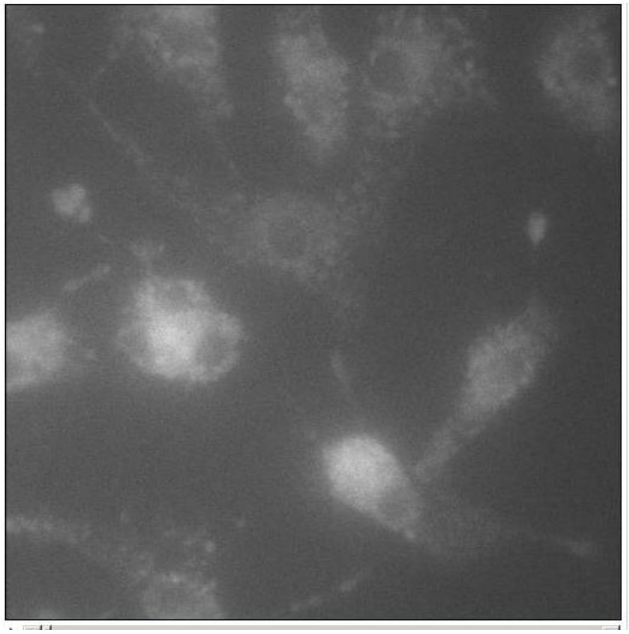

Figure 14: NRVMs infected at MOI 1 showing possible focal adhesions as punctuate dots using widefield microscopy. Focal adhesions were confirmed through immunofluorescence.

Discussion:

Stamping-Optimization:

To begin developing this model, we sought to reproduce and optimize the technique detailed by McDevitt, et al., 2001. Initially, we were storing our laminin stamped plates at 4 ℃ and found trouble maintaining patterning even after imaging successful laminin transfer as seen in Fig. 5E. After further research we found that laminin polymerizes at 35 ℃ and breaks down into monomers at 4 ℃ (Yurchenco, et al. 1985). Initially we had carried out all stamping at room temperature, after reading the literature we decided to incubate laminin at 37 ℃ while laminin incubated on the stamp and during the stamp-substrate phase. This led to crystallization of laminin across the glass coverslip (Fig. 5D). We found incubating laminin while on stamps while at room temperature and then incubating at 37 ℃ during glass contact yielded the most consistent, clean patterning (Fig. 5E).

ECM proteins vary in the amount of protein needed to allow cells to successfully adhere. Engler et al. 2008 and Pelham and Wang 1997 used 0.2mg/ml collagen cross-linked to polyacrylamide gels. We had been using 30μg/ml of laminin. To ensure we used the proper amount of laminin we varied the concentration of laminin from 30 to 100 μg/ml and found that increasing the concentration led to crystallization of laminin polymers and nearly complete loss of patterning (Fig 5C).

Transferring this stamping method to PA gels required additional optimization.

Micropatterning on PA gels had been done previously (A. J. Engler, et al. 2004) using a glass stamp and a fluidic micropatterning technique. We sought to directly transfer our optimized stamping technique to the PA gel. Initially successful (Fig. 5H), we encountered problems obtaining the same level of consistency of patterning we had initially experienced on glass and gels. We attempted to vary the stiffness of the PDMS stamp, mimicking a glass stamp as used by the Engler group, but found that it did not fix the problem. We varied the laminin concentration again, but still failed to obtain patterning of cells, or any adherence of cells. We soon discovered that the SANPAH is required to be stored at -80 ℃, while we had stored it at 4 ℃. New SANPAH was obtained, aliquoted, and stored according to instructions and used fresh aliquots for each gel activation. This solved our problem immediately and we have continued to work on reproducibility and consistency in our patterning on PA gels.

Cells: Maintenance/Density-

After becoming consistent in our stamping technique, we next aimed to determine the proper cell density to plate. We had found previously that seeding too many or too few cells disrupted patterning. Too many cells leads to cells bridging the gap between lanes, aligning parallel on the lane, or many dead cells that could potentially pollute the media, causing healthy cells to die due to an increase in toxicity within the media. While too few cells leads to a decrease in likelihood of cardiofilament formation with cells being spaced too far apart to make the necessary connections to allow NRVMs to differentiate into cardiofilaments for example the spacing seen in Fig. 8C. We found the optimal density to be 250,000 cells/1.54cm^2. This allowed a higher probability of

cardiofilament formation without cells bridging or cell death causing media toxicity. Next we sought to increase the longevity of our cultured cells to allow us adequate time to experiment on healthy cells. Changing whole dish media was causing cells to die off and stop contracting 7-10 days post plating. This caused severe limitations to our experiments. While in culture, cells begin to secrete proteins into the media after plating, such as healthy growth factors. By removing all the media at each media change we were likely shocking the cells and removing vital healthy factors from the media. We began removing and replenishing just half the media at each media change and found that cells remained contractile until day 30 (longest observed). We also found that at the initial 6 hour media change, we needed to rinse the cells with warm media to ensure nearly complete removal of dead cells. The ability to maintain healthy, contractile cells will increase the number of experiments we can do.

Cardiofilament Development on Glass and PA Gels:

Our system encourages NRVMs to differentiate into "cardiofilaments", which exhibit an organized sarcomere and maintain their ability to make strong ECM contacts. We first needed to prove that our system allowed NRVMs to develop an organized sarcomere and connection between cells that will allow mechanical signals to propagate along the length of the cardiofilament. Initially, as we pursued glass substrates, we found that by day 5 NRVMs began to express excess connexin-43 (Fig. 7E) and observed excellent sarcomere formation by day 3 (Fig. 7D) with nice connections between cells. As we turned to using PA gels, we needed to determine when NRVMs on PA developed organized sarcomere and compare our results to those we had seen on glass. We found

that at day 3 (Fig. 7A) had no organized sarcomere, but by day 5 sarcomere had clearly developed and were maintained through day 7 (Fig. 7B & C). We also found that NRVMs maintained contractility up to day 20 (longest observed) and will have to carry out additional experiments to determine if the cells maintain their sarcomere or begin to deteriorate at we had seen previously on glass. This provided us the ability to do more experiments on these cells as they are healthier for longer periods of time. It will be interesting to fix and stain cells over longer period of time to determine how long these cells maintain their sarcomeres. This demonstrated that cells on PA gels are healthier and less likely to express stress proteins and fibers that could affect our studies. These two substrates will give us the ability in the future to compare healthy contractile cells to cells resembling those post-infarct. It presents intriguing possibilities for us to explore as we optimize our methodology further.

NRVMs deteriorating on glass is unsurprising with recent work done by Engler et al 2008, which shows that cells on a rigid substrate such as glass tend to resemble cardiomyocytes after infarction and cells themselves begin to deform rather than deform their substrate such as when using a polyacrylamide gel. It will be of interest to carry out further experiments analyzing expression of fetal genes to determine if cells on glass are reverting back to this state and exacerbating hypertrophy. It will also be interesting to determine which form of myosin heavy chain is expressed in the cells depending on the substrate. We need to carry out these experiments to state confidently that we have created cardiofilaments that are similar to adult cardiac tissue.

Talin Adenovirus:

Being able to visualize integrin activation in real time is key to our project. To do this we first needed to find a protein that bound activated integrin but did not activate the integrin. Talin became an integral part of this work after Bouaouina, et al., 2008 showed that isolated talin head domain is able to bind, but does not activate β1 integrin tails. This key piece of research also made it imperative that we use laminin as opposed to fibronectin. Fibronectin activates β3 integrin tails, as does isolated talin head domain, which would lead to endogenous activation of integrins. We were able to successfully amplify selected talin constructs (Fig. 10) and ligate into our vector containing GFP to create our talin-GFP fusion protein. We then transfected C2C12 cells with this DNA to determine which constructs of talin colocalize with integrin at focal adhesions. We found that, as had been seen in previous literature, the talin head domain, F2F3, and F3 subdomains colocalized with integrin (Fig. 11). We were able to digest F2F3 out of our vector and ligate into pShuttle-CMV shuttle vector and recombined into the pAdEasy viral backbone (Fig. 12).

Virus was then used to infect F2F3-GFP fusion protein into isolated NRVMs and cells were imaged using confocal microscopy and live cell imaging with real-time widefield imaging. NRVMs grown on PA gels were fixed and stained to determine if the fusion protein was able to colocalize with integrin in NRVMs. We found that F2F3-GFP protein was able to clearly localize with integrins at focal adhesions (Fig. 13C & F & I). Showing that our fusion protein is able to localize with integrins in fixed cells, we then utilized real-time widefield microscopy and live cell imaging. Infected NRVMs imaged under real-time microscropy showed possible focal adhesions (Fig. 14). Further

experiments need to be done to determine how changes in acto-myosin forces affect the intensity of GFP at the focal adhesions, which should correlate with an activation or dispersal of integrin and the cell membrane. Currently, a control virus expressing GFP is being amplified and purified for use in future experiments to control for viral effects on the cell.

Summary and Future Direction:

In the future we need to optimize this final step in our system. Live cell imaging is difficult and will require further work to create reproducibility and consistency in our videos. We also need to optimize our pacing technique, conditions to improve length of time cells are contractile in the chamber (currently <30mins), auto-focusing during the movies and controlling the flow rate (i.e. should it be constant or stop and go?).

We have the opportunity to explore the difference between NRVMs on a substrate similar to healthy cardiac tissue and those on a substrate resembling heart tissue post-infarction. In the future, we need to continue to increase the reproducibility of this model through continued diligence towards optimizing our stamping technique on polyacrylamide gels. We also need to begin to address the many variables real-time imaging presents. We have the opportunity to create a system that other researchers can use in their endeavors and will continue to perfect this technique. Our research will be among the first to begin to understand how changes in force generation affects integrin activation and in the future hypertrophy. We have successfully created a model system we can use to study integrin activation and how altered sarcomere contractility affects integrin activation. The next step is to obtain more videos of infected cardiomyocytes

and analyze changes in focal adhesion intensity overtime in response to altered sarcomere contractility.

Bibliography

Agrawal, Rohini, Neeraj Agrawal, Chintan Koyani, and Randhir Singh. "Molecular targets and regulation of cardiac hypertrophy." *Pharmacological Research*, November 2009: 269-280.

Arnaout, M.Amin, Simon Goodman, and Jian-Ping Xiong. "Structure and mechanics of integrin-based cell adhesion." *Current Opinions in Cell Biology* 19(5) (2007): 495-507.

Barry, Sean P, Sean M Davidson, and Paul A Townsend. "Molecular regulation of cardiac hypertrophy." *The International Journal of Biochemistry and Cell Biology*, February 2008: 2023-2039.

Beningo, K.A., M. Dembo, I Kaverina, J.V. Small, and Y.L Wang. "Nascent focal adhesions are responsible for the generation of strong propulsive forces in migrating fibroblasts." *Journal of Cell Biology* 153 (2001): 881-888.

Bennett, JS, and G Vilaire. "Exposure of platelet fibrinogen receptors by ADP and epinephrine." *Journal of Clinical Investigation* 64 (1979): 1391-1401.

Bloom, S, VG Lockard, and M Bloom. "Intermediate filament-mediated stretch-induced changes in chromatin: a hypothesis for growth initiationin cardiac myocytes." *Journal of Molecular Celll Cardiology* 28 (1996): 2123-2127.

Bouaouina, Mohamed, Yatish Lad, and David A Calderwood. "The N-terminal domains of talin cooperate with the phosphotyrosine binding-like domain to activate beta1 and beta3 integrins." *Journal of Biological Chemistry* 283 (2008): 6118-6125.

Byzova, TV, et al. "A mechanism for modulation of cellular responses to VEFG: activation of integrins." *Molecular Cell* 6 (2000): 851-860.

Calderwood, David A, Roy Zent, Richard Grant, Jasper G. rees, Richard O. Hynes, and Mark H. Ginsberg. "The talin head domain binds to integrin beta subunit cytoplasmic tails and regulates integrin activation." *Journal of Biological Chemistry* 274 (1999): 28071-28074.

Carman, CV, and TA Springer. "Integrin avidity regulation: are changes in affinity and conformation underemphasized?" *Current Opinions in Cell Biology* 15 (2003): 547-556.

Choquest, D, D Felsenfeld, and M Sheetz. "Extracellular matrix rigidity causes strengthening of integrin-cytoskeleton linkages." *Cell* 88 (1997): 39-48.

Clerk, Angela, et al. "Signaling Pathways Mediating Cardiac Myocyte Gene Expression in Physiological and Stress Responses." *Journal of Cellular Physiology*, 2007: 311-322.

Cukierman, E, R Pankov, R Stevens, and K.M. Yamada. "Taking cell0matrix adhesions to the third dimension." *Science* 294 (2001): 1708-1712.

Dabiri, G.A., J.C. Ayoob, K.K. Turnacioglu, J.M. Sanger, and J.W. Sanger. "Use of green fluorescent proteins linked to cytoskeletal proteins to analyze myofibrillogenesis in living cells." *Methods in Enzymology* 302 (1999): 171-186.

Discher, D.E., P.A. Janmey, and Y.L. Wang. "Tissue cells feel and respond to the stiffness of their substrate." *Science* 310 (2005): 1139-1143.

Dorn, Gerald, Jeffrey Robbins, and Peter Sugden. "Phenotyping Hypertrophy." *Circulation Research*, 2003: 1171-1175.

Du, A, J.M. Sanger, K.K. Linask, and J.W. Sanger. "Myofibillogenesis in the first cardiomyocytes formed from isolated quail precardiac mesoderm." *Developmental Biology* 257 (2003): 382-394.

Engler, A.J., L. Bacakova, C. Newman, A. Hategan, M. Griffin, and D. Discher. "Substrate compliance versus ligand density in cell on gel responses." *Biophys J.* 86 (2004a): 617-628.

Engler, Adam J, Maureen A Griffin, Shamik Sen, Carsten G. Bonnemann, H. Lee Sweeney, and Dennis E. Discher. "Myotubes differentiate optimally on substrates with tissue-like stiffness: pathological implicaitons for soft or stiff microenvironments." *Journal of Cell Biology* 166 (2004): 877-887.

Engler, Adam J., et al. "Embryonic cardiomyocytes beat best on a matrix with heart-like elasticity: scar-like rigidity inhibits beating." *Journal of Cell Science* 121 (2008): 3794-3802.

Engler, Adam J., Maureen A. Griffin, Shamik Sen, Carsten G. Bonnemann, H. Lee Sweeny, and Dennis E. Discher. "Myotubes differentiate optimally on substrates with tissue-like stiffness: pathological implications for soft or stiff microenvironments." *Journal of Cell Biology* 166 (2004): 877-887.

Hemmings, L, et al. "Talin contains three actin-binding sites each of which is adjacent to a vinculin-binding site." *Journal of Cell Science* 109 (1996): 2715-2726.

Hughes, PE, and M Pfaff. "Integrin affinity modulation." *Trends in Cellular Biology* 8 (1998): 359-364.

Hynes, RO. "Integrins: a family of cell surface receptors ." *Cell* 48 (1987): 549-554.

Ingber, D. "Integrins as mechanochemical transducers." *Current Opinions in Cell Biology* 3 (1991): 841-848.

Johnston, Rebecca K., Sundaravadivel Balasubramanian, Harinath Kasiganesan, Catalin F. Baicu, Michael R. Zile, and Dhandapani Kuppuswamy. "Beta3 integrin-mediated

ubiquitination activates survival signaling during myocardial hypertrophy." *FASEB Journal* 23 (2009): 2759-2771.

Kira, Y, T Nakaoka, E Hashimoto, I Sekine, F Okabe, and S Asano. "Effect of long-term cyclinc mechanical load on protein synthesis and morphological changes in cultured myocardial cells from neonatal rats." *Cardiovascular Drugs Therapy* 8 (1994): 251-262.

Kira, Y., PJ Kochel, EE Gordon, and HE Morgan. "Aortic perfusion pressure as a determinant of cardiac protein synthesis." *American Journal of Physiology* 246 (1984): 247-258.

Komuro, I, T Kaida, and Y Shibazaki. "Stretching cardiac myocytes stimulates protooncogene expression." *Journal of Biological Chemistry* 265 (1990): 3595-3598.

Komuro, Issei. "Molecular Mechanism of Mechanical Stress-induced Cardiac Hypertrophy." *Japan Heart Journal,* 2000: 117-129.

Liddington, RC, and MH Ginsberg. "Integrin activation takes shape." *Journal of Cell Biology* 158 (2002): 833-839.

Mangeat, P, C Roy, and M Martin. "ERM proteins in cell adhesion and membrane dynamics." *Trends Cell Biol* 9 (5) (1999): 187-192.

Mann, DL, RL Kent, and IVG Cooper. "Load regulation of the properties of adult feline cardiomycytes: growth induction by cellular deformation." *Circulation Research* 64 (1989): 1079-1090.

McDevitt, Todd C, et al. "In vitro generation of differentiated cardiac myofibers on micropatterned laminin surfaces." *Journal of Biomedical Materials Research* 60 (2001): 472-470.

Moes, M, et al. "The integrin binding site 2 (IBS2) in the talin rod domain is essential for linking integrin beta subunits to the cytoskeleton." *Journal of Biological Chemistry* 282 (2007): 17280-17288.

Muguruma, M, S Nishimuta, Y Tomisaka, T Ito, and S Matsumura. "Organization of the functional domains in membrane cytoskeletal protein talin." *Journal of Biochemistry* 117 (5) (1995): 1036-1042.

Nadal-Ginard, Bernardo, Jan Kajstura, Annarosa Leri, and Piero Anversa. "Myocyte Death, Growth, and Regeneration in Caridac Hypertrophy and Failure." *Circulation Research*, 2003: 139-150.

Narula, J., et al. "Apoptosis in myocytes in end-stage heart failure." *N. England Journal of Medicine* 335 (1996): 1182-1189.

Pelham, R.J., and Y.L. Wang. "Cell locomotion and focal adhesions are regulated by substrate flexibility." *Proc. Natl. Acad. Sci.* 94 (1997): 13661-13665.

Peyton, S.R., and A.J. Putnam. "Extracellular matrix rigidity governs smooth muscle cell motility in a biphasic fashion." *Journal of Cell Physiology* 204 (2005): 189-209.

Ratnikov, B.I., A.W. Partridge, and M.H. Ginsberg. "Integrin Activation by Talin." *Journal of Thrombosis and Haemostasis* 3 (2005): 1783-1790.

Rees, D.J., S.E. Ades, S.J. Singer, and R.O. Hynes. "Sequence and domain structure of talin." *Nature* 347 (1990): 685-689.

Ruwhof, Cindy, and Arnoud van der Laarse. "Mechanical stress-induced cardiac hypertrophy: mechanisms and signal transduction pathways." *Cardiovascular Research* 47 (2000): 23-37.

Sadoshima, J, L Jahn, T Takahashi, TJ Kulik, and S Izumo. "Molecular characterization of the stretch-induced adaptation of cultured cardiac cels. An invitro model of load-induced cardiac hypertrophy." *Journal of Biological Chemistry* 267 (1992): 10551-10560.

Schwartz, K., D de la Bastie, P Bouveret, P Oliviero, S Alonso, and M Buckingham. "alpha-skeletal muscle actin mRNAs accumulate in hypertrophied adult rat hearts." *Circulation Research* 59 (1986): 551-555.

Shake, J.G., et al. "Mesenchymal stem cell implantation in a swine myocardial infarct model: engrafment and functional effects." *Ann. Thorac. Surg.* 73 (2002): 1919-1925.

Shimaoka, M, J Takagi, and TA Springer. "Conformational regulation of integrin structure and function." *Annual Rev Biophysical Biomolecular Structure* 31 (2002): 485-516.

Tanentzapf, G, and NH Brown. "An interaction between integrin and talin FERM domain mediates integrin activation but not linkage to the cytoskeleton." *Nat Cell Biol* 8 (6) (2006): 601-606.

Vandenburg, HH, R Solerssi, J Shanksky, JW Adams, SA Henderson, and J Lemaire. "Response of neonatal rat cardiomyocytes to repetitive mechanical stimulation in vitro." *Ann NY Acad Sci* 752 (1995): 19-29.

Wang, H.B., M. Dembo, and Y.L. Wang. "Substrate flexibility regulates growth and apoptosis of normal but not transformed cells." *American Journal of Physiology Cell Physiology* 279 (2000): 1345-1350.

Wang, N, et al. "Cell prestress I. Stiffness and prestress are closely associated in adherent contractile cells." *American Journal of Physiology Cell Physiology* 282 (2002): 606-616.

Wenker, D, et al. "A mechanistic role for cardiac myocyte apoptosis in heart failure." *Journal of Clinical Investigation* 111 (2003): 1497-1504.

Yurchenco, Peter D., Effie c. Tsilibary, Aristidis S. Charonis, and Heinz Furthmayr. "Laminin Polymerization in Vitro." *Journal of Biological Chemistry* 260 (1985): 7636-7644.